Journal of Civil Engineering and Architecture 10 (2016) 743-754
doi: 10.17265/1934-7359/2016.07.001

Damage of Historical Stone Masonry Buildings: Combined Effects of Spatial Variability of Stone Properties and Environmental Conditions

Naima Belayachi and Dashnor Hoxha
Université d'Orléans, INSA-CVL, PRISME, EA 4229, Orléans 45072, France

Abstract: The everyday fluctuations of temperature and humidity lead to fluctuation of stress on the stones constituting many constructions and produce in long term some kinds of fatigue damage. This paper investigates the combined role of stone properties variability and environmental conditions on the generation and the amplification of stress variation and fatigue. Thus, the randomness and spatial variability of the mechanical, thermal and hydraulic properties are taken into account in a finite elements model of typical stone wall masonry of Chambord Castle. The quantification of the impact of this spatial variability on the variability of generated stress is performed.

Key words: Masonry structures, fatigue, damage, spatial variability, thermo-hydro-mechanical coupling.

1. Introduction

Damage and deterioration of historical masonry buildings are complex phenomena whose understanding is yet nowadays a field of intensive various mechanisms such as salt enhanced weathering due to salt crystallization in pores [1], atmosphere pollution, stone wetting and drying [2]. Severe frost or heating are evoked to be of major impact on ageing and deteriorating of stone buildings [3]. A large number of experimental works were dedicated to reproduce the in-situ environmental conditions in order to identify and quantify deterioration mechanism and their combined effects [4, 5]. Damage, cracking and their evolution in historical masonry building were assessed in-situ through an approach combining nondestructive techniques and nonlinear numerical simulations [6-8]. Other authors have used a long-term viscoelastic creep model [9] to predict the damage evolution. They observed, that the difference in strength and stiffness lead to a stress redistribution and stress concentrations which could be in the origin of initiation and/or acceleration of masonry damage. Generally, all studies led to the conclusion that the damage of stone masonry buildings results from a combination of "natural" stress due to gravity and/or horizontal loads with other long term phenomena, such as chemical, thermal or hydrous-enhanced stress.

In a previous work, the authors addressed the impact of daily variation of temperature and humidity on the damage of the white tuffeau stone [10], broadly used in construction of so called "*Chateaux de la Loire*" castles. The THM (thermo-hydro-mechanical) analysis for unsaturated porous media used in that work to study the behavior of a stone wall showed that the everyday fluctuation of temperature and humidity induced a stress field whose fluctuations are strong enough to induce a fatigue of white tuffeau stone. In this analysis, spatially uniform properties have been considered for the stone. The spatial natural variability of stone properties from point to point of a wall not only could explain why for the same conditions the stone deterioration will take place only on some parts of a

Corresponding author: Naima Belayachi, Dr., associate professor, research fields: non-linear mechanical behaviour, micro-macro modeling, coupling modelling and thermo-hydro-mechanical material characterization.

wall, but also it could be a factor for amplification of stress fluctuation itself and initiation of damage [11]. Many authors consider that the stress field fluctuation, both spatial and temporal, is a major factor of fatigue enhanced cracks [10, 12, 13]. In Ref. [13], the authors concluded that the failure could take place earlier than predicted by mean field theories because of fluctuations of the stress state. The stress fluctuation is mentioned also as a principal crack growth mechanisms of materials under uniaxial compression [14].

The principal origin of stress fluctuation on heterogeneous materials as stones is the spatial distributions of minerals constituting the stone, porous microstructure, grains boundaries and so on [15]. To understand the behaviour of stone masonry walls, and evaluate the effect of different parameters like mortar joints, nature and shape of the stones, several experimental investigations are performed by using destructive and non-destructive testing [16-18].

Following the above mentioned work [10] on THM modeling of stone wall behavior, in this paper the effort is focused on the influence of the spatial variability of stone properties on the stress fluctuations and consequently on the deterioration of historical buildings. For that, the authors use the same mathematical and physical framework as in Ref. [10] but some key properties are supposed to be randomly distributed. The stress field is then characterized in respect with their spatial fluctuation and related to the heterogeneous nature of the tuffeau stone as a potentially mechanism on the damage and deterioration.

2. Thermo-Hydro-Mechanical Heterogeneity as a Source of Local Stress Fluctuation

This paper firstly describes the theoretical and numerical framework of modeling used to predict the stress variation due to everyday variation of temperature and humidity on the surface of a stone wall. The geometrical model used in this study is much similar to that used in Ref. [10] and represents a wall stone masonry with mortar joint mimicked stone walls of Chambord Castle. Then the heterogeneity of stress due to variation of meteorological variations and spatial variability of material properties is estimated through the variance between the homogeneous and heterogeneous case. Likewise some previous works [10, 19, 20], the numerical models and tools developed for geomaterials are used for modeling stones behavior considered as partially saturated soft rocks with a solid phase and liquid (water) and gaseous phases (dries air and water vapor) contained in pores system [21].

2.1 Thermo-Hydro-Mechanical Model

This paper briefly presents in this section the essential of equations for coupled THM model. The interested reader could find more details in Ref. [21].

The well-known effective stress taking into account the effect of temperature and relative humidity is done as follow:

$$\underline{\underline{\sigma}}' = \underline{\underline{\sigma}} + b\pi\underline{\underline{\delta}} + 3\alpha K\Delta T\underline{\underline{\delta}} \qquad (1)$$

where, the second ($b\pi\underline{\underline{\delta}}$) and third terms ($3\alpha K\Delta T\underline{\underline{\delta}}$) in Eq. (1) present coupling terms respectively for hydro mechanical and thermo mechanical behavior respectively through Biot's coefficient $b = 1 - K/K_s$ and thermal expansion coefficient α (supposed for the sake of simplicity as being isotropic). The parameters K and K_s are bulk modulus of the drained medium and solid grains, respectively. In the case of saturated media, π represents interstitial pressure but for the unsaturated media it is a function of liquid saturation S_{lq} and capillary pressure P_c (difference of the gaseous and liquid pressure $P_C = P_g - P_l$) [21]:

$$\pi = \begin{cases} \int_{S_{lq}}^{1} S_{lq}(P_C)\,dP_C & \text{if } S_{lq} < 1 \\ P_l & \text{if } S_{lq} > 1 \end{cases} \qquad (2)$$

The function $S_{lq}(P_C)$ represents the isothermal sorption curve of the material which must be evaluated by experimental tests. The tuffeau sorption curve is that

used in Ref. [10] and can be approximated by an empirical Van Genuchten expression:

$$S_{lq}\left(P_c\right)=\left[1+\left(\frac{P_C}{P_r}\right)^n\right]^{\frac{1-n}{n}} \quad (3)$$

where, P_r (stress units) and n (dimensionless) are two fitting parameters.

For a given air humidity, the capillary pressure P_c can be evaluated from the relative humidity by considering the perfect gases law (Kelvin's law):

$$P_C=\frac{\rho_l\cdot R\cdot T}{M_l^{ol}}\ln\left(Hr\right) \quad (4)$$

where, R and M_l^{ol} are, respectively, the constant of perfect gases and the molar mass of water, and Hr is relative humidity.

The advection of gaseous and liquid phase is governed by generalized Darcy's law:

$$\frac{\underline{M}_j}{\rho_j}=-\lambda_j\,\underline{\mathrm{grad}}\left(P_j\right)\qquad j=\mathrm{liquid},\mathrm{gas} \quad (5)$$

where, the flux vector M_j is propotional to the effective hydraulic conductivity λ_j in unsaturated media of each phase (liquid, gas). This hydraulic conductivity is defined as:

$$\lambda_j=\frac{k_{in}\cdot k_j^{rel}\left(S_l\right)}{\mu_j}\qquad j=\mathrm{liquid},\mathrm{gas} \quad (6)$$

where, k_{in} is the intrinsic permeability and k_j^{rel} is the relative permeability, a limited value function of liquid saturation S_{lq} taking values between 0 and 1.

The diffusion of the vapor in the mixture of gases (air and vapor) is described by Fick's law:

$$\frac{\underline{M}_v}{\rho_v}=-F\ \underline{\mathrm{grad}}\left(C_{vp}\right) \quad (7)$$

where, C_{vp} and F are respectively concentration of vapor in gaseous phase and Fick's coefficient.

To complete the transfer equations, the heat transfer is governed by Fourier's law:

$$\underline{q}=-\lambda_T\ \underline{\mathrm{grad}}\left(T\right) \quad (8)$$

where, $\underline{q}$ is the thermal flux and λ_T is thermal conductivity.

In this study, the proposed modeling consists in combining the heterogeneous stone nature and variation of climatic conditions to evaluate the effective stresses. So a linear elastic model is considered to describe the behaviour of both tuffeau stone and mortar to avoid other nonlinear mechanisms.

The tuffeau stone wall is modelled in plane strain configuration by a vertical cut perpendicular to the stretch of the wall. The thickness of this cut is of 80 cm and the height is 15 m corresponding to historical castle walls (Fig. 1). In order to avoid the effects of boundaries, the authors focus attention on a stone block comprised between two mortar joints, while the other parts of walls are considered as an equivalent continuum media with average properties of stone blocks and mortars (Table 1). A perfect adherent interface is assumed between the stone block and mortar. The initial temperature and relative humidity are considered uniform in the wall and equal to T_0 = 20 °C and RH_0 = 53%, respectively. The effect of initial state has been studied in previous investigation [10].

The Fig. 1 shows the boundary conditions on the outdoor surface (right boundary), the indoor one (left boundary) and the finite element mesh. The temperature and relative humidity applied on the outdoor surface are obtained by a statistical analysis of time series of meteorological data around Chambord Castle.

For the thermo-hydro-mechanical modeling, several material parameters are necessary.

The thermo-hydro-mechanical description identifies several material parameters. For the tuffeau stone and joint mortar of Chambord Castle, in previous experimental investigation the material properties are available [4]. Some of mortar parameters like the thermal expansion coefficient and isothermal sorption curve are identified by an inverse analysis based on the in-situ measured data. The relative liquid permeability is chosen as a third power function.

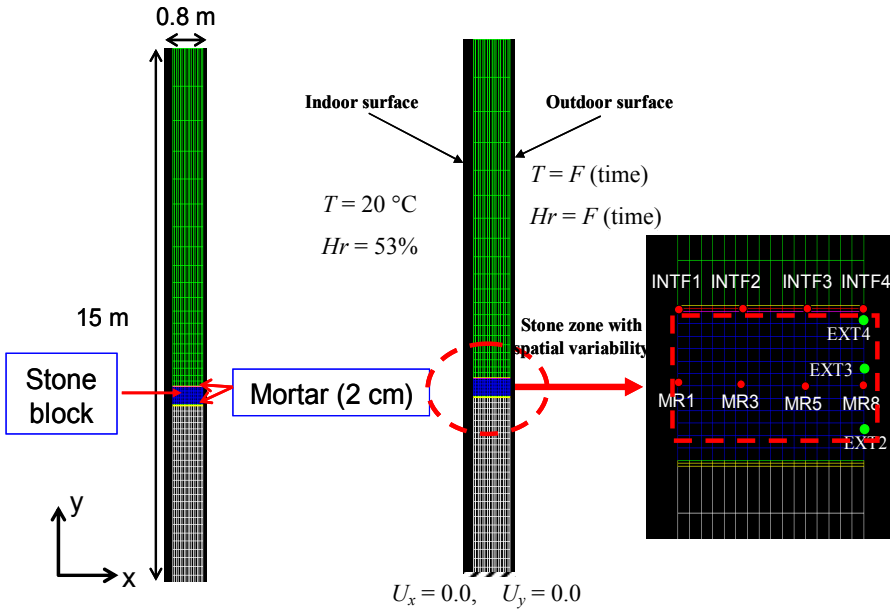

Fig. 1 Geometrical finite element model and boundary conditions.

Table 1 Material parameters for tuffeau stone and mortar.

	Parameter	Tuffeau stone	Mortar
Mechanical parameters	Young's modulus (E (MPa)) Poisson's coefficient (ν) Mass density (ρ (kg·m^{-3}))	1,953 0.19 1,300	1,604 0.2 1,240
Hydraulic parameters	Intrinsic permeability (k_{int} (m^2)) Porosity (ϕ (%))	1×10^{-13} 42	0.2×10^{-13} 50
Thermal parameters	Thermal conductivity (λ (W·m^{-1}·K^{-1})) Heat capacity (C_p (J·kg^{-1}·K^{-1}))	0.56 830	0.56 830
Coupling thermo-hydro-mechanical parameters	Biot's coefficient (b)	0.5	0.5
	Thermal expansion coefficient (α (K^{-1}))	6.0×10^{-6}	12×10^{-6}
	Isothermal sorption curve (Eq. (3)) P_r (MPa) n	0.013 1.37	0.013 1.37

The different parameters used to perform the numerical calculations for the tuffeau stone and joint mortar of Chambord walls are given in Table 1.

2.2 Spatial Variability of Stone Properties

This paper presents in this section the methodology used to describe spatially heterogeneous damage zones in stone block based on the calculation of the variance. The estimation of the stress variance is carried out on results of the numerical simulations performed once using a homogeneous stone and then a heterogeneous one. Usually, the variance at two different locations is used to study the influence of heterogeneous fault zones on fluid flow of rocks [22, 23] or weathering of natural stones [24].

In order to take into account the spatial variability of the stone, several realizations of normal distribution for three parameters (Young's modulus, thermal expansion parameter and intrinsic permeability) are performed. Histograms showing the parameter distribution are presented in Fig. 2.

The mean values of distributions coincide with those of experimental measured properties: for Young's modulus the mean value is 1,953 MPa, while the mean value of permeability and thermal expansion coefficient are 10^{-13} m^2 and 6×10^{-6} K^{-1}, respectively.

To effectively integrate a spatially heterogeneous material in the modeling, the values of these three

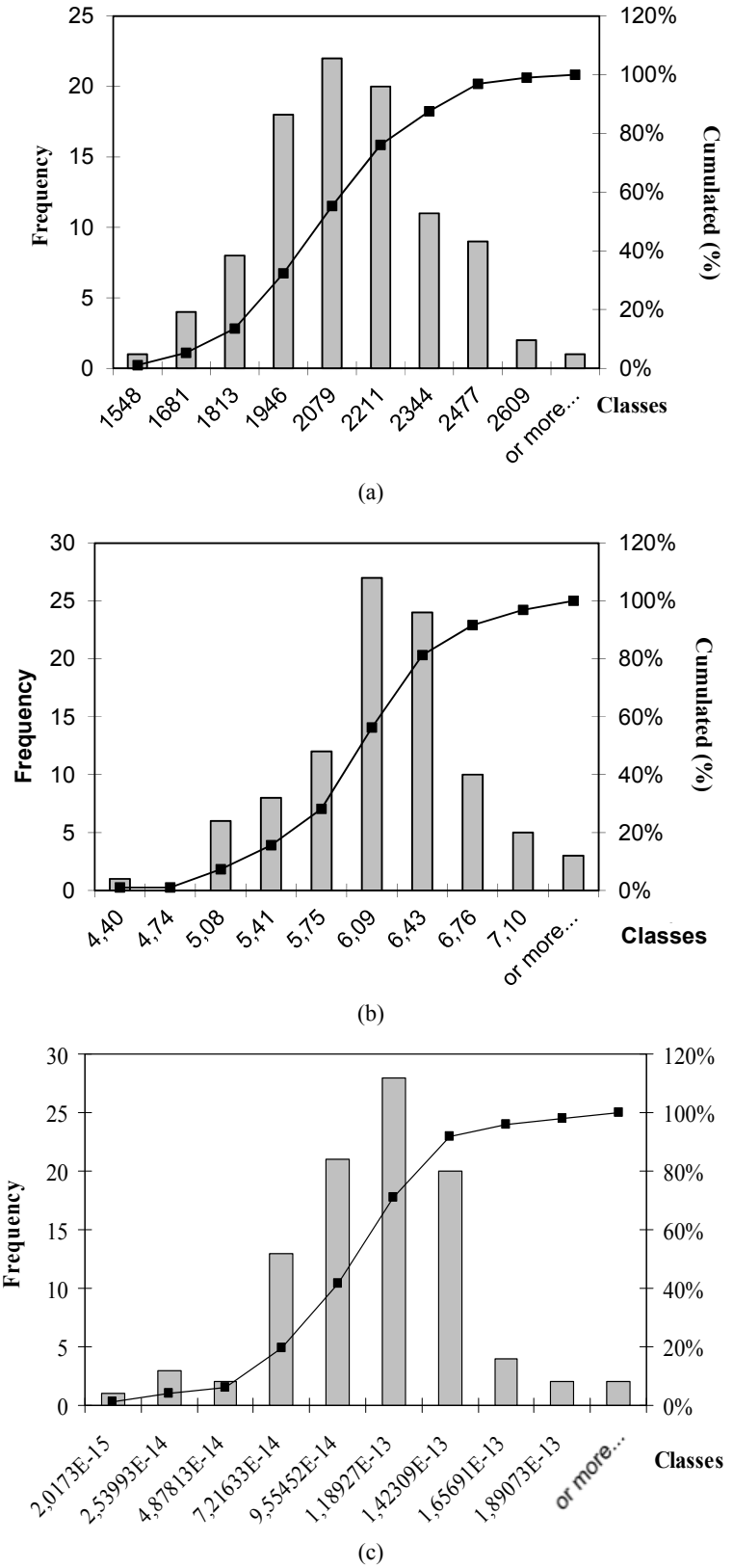

Fig. 2 Histograms of normal distribution of: (a) Young's modulus E (MPa); (b) thermal expansion coefficient α (K^{-1}); and (c) permeability K (m^2).

parameters are supposed uncorrelated and following normal distributions. The values of these parameters obtained by independent realizations are affected in random way on Gauss points on the zone representing the tuffeau stone block (Fig. 1). An example of the contour map of properties distribution is given in Fig. 3 for Young's modulus and thermal expansion coefficient. Similar contours are obtained for permeability. With the aim of comparing the effect of the heterogeneity of each parameter on the stress fluctuation, several simulations were performed affecting as random distribution one, two or the three of properties and keeping others as homogeneous.

3. Results and Discussions

The THM simulations were performed using Code_Aster (EDF) finite element tool taking into account the everyday fluctuations of temperature and humidity during one year. For the comparative analyses the effective stresses for 30 and 366 days at each node of the stone block are calculated. Then, the normalized variance is estimated using the following Eq. (11):

$$\psi = \frac{\Delta\sigma - \Delta\sigma_m}{\Delta\sigma_m} \quad \text{with} \quad \begin{cases} \Delta\sigma = \sigma_{\text{spatial variability}} - \sigma_{\text{homogeneous}} \\ \Delta\sigma_m \text{ mean value of } \Delta\sigma \end{cases} \tag{11}$$

According to x axes and y axes, the contour maps of this normalized variance are carried out by using gridding and 3D contouring capabilities of surfer code. Fig. 4 represents the contour maps of stress

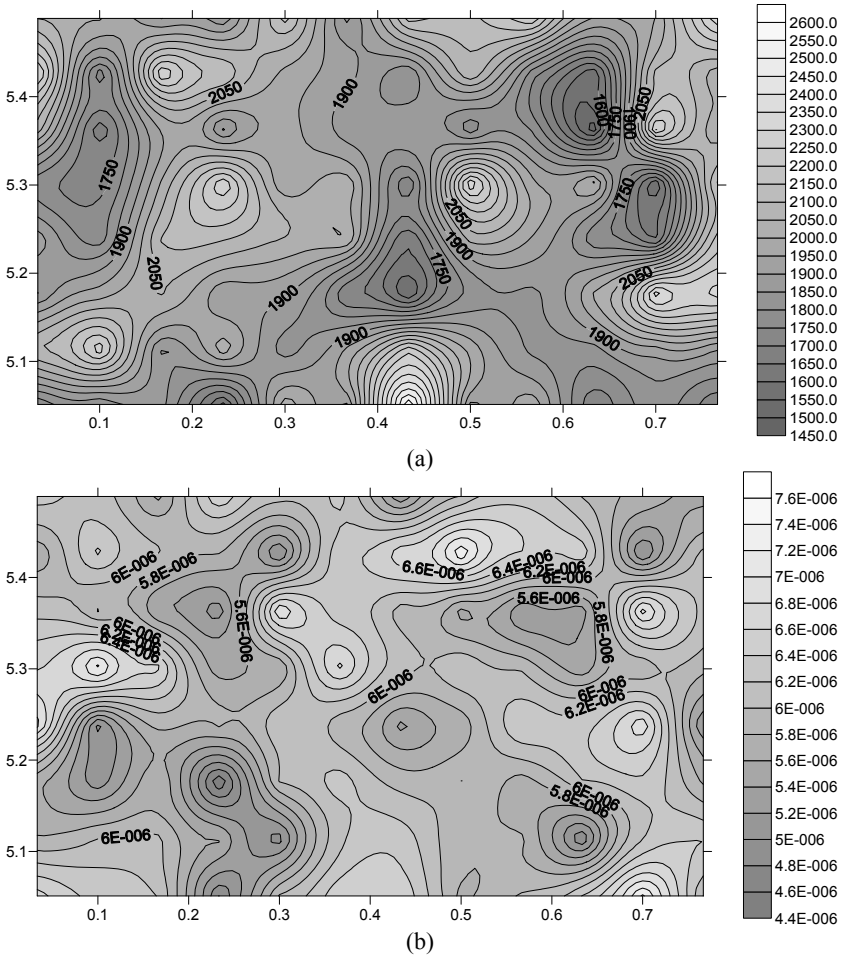

Fig. 3 Random distributions of the stone properties affected at the stone mesh: (a) Young's modulus; (b) thermal expansion coefficient.

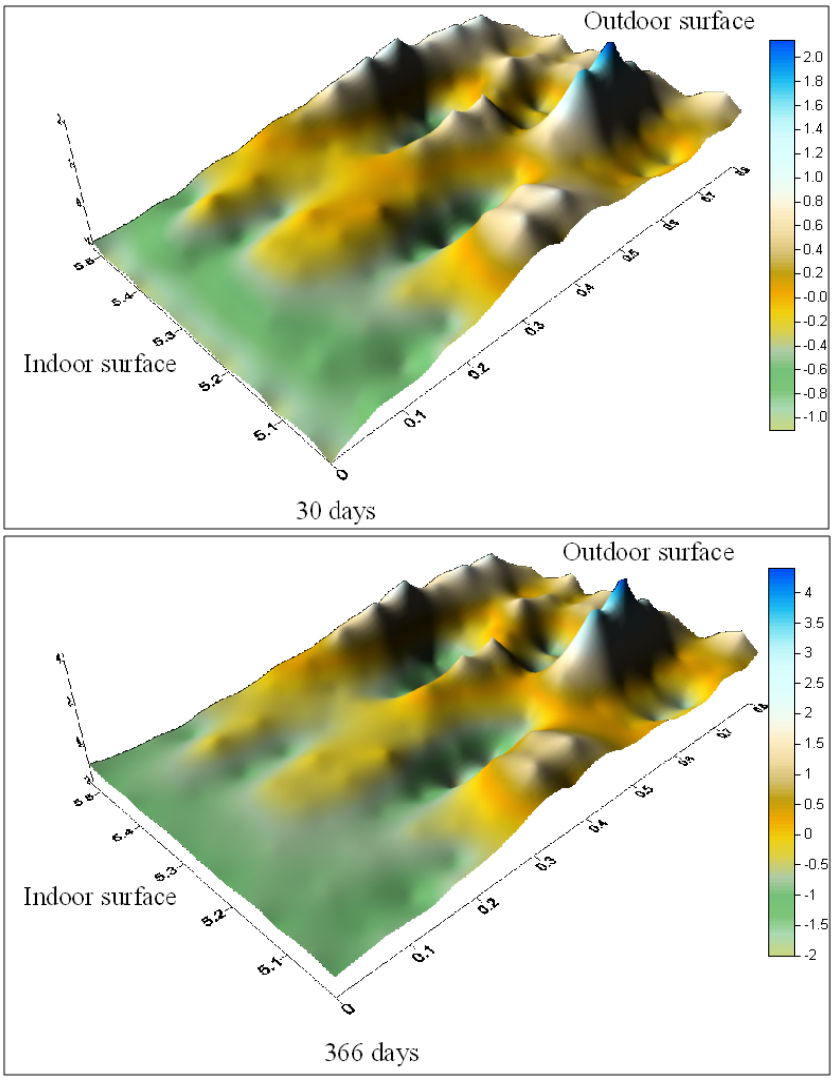
Outdoor surface
Indoor surface
30 days
Outdoor surface
Indoor surface
366 days

(a)

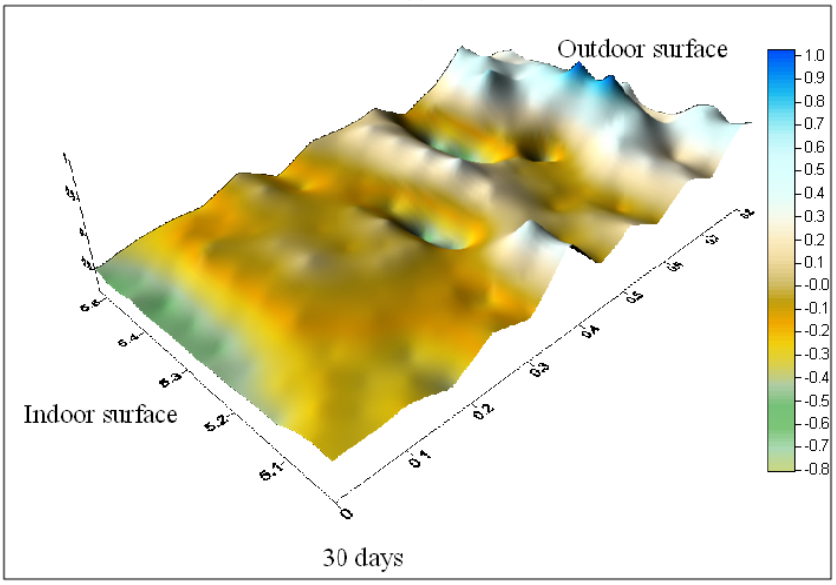
Outdoor surface
Indoor surface
30 days

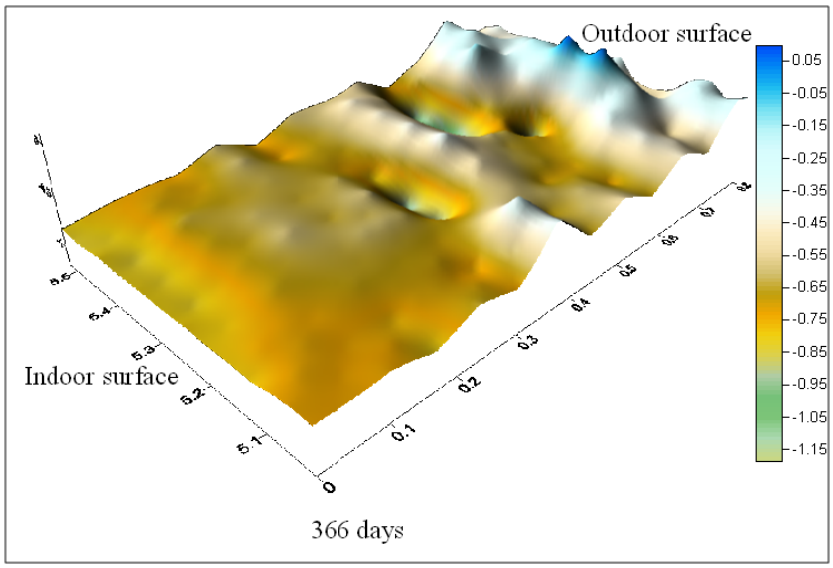

(b)

Fig. 4 Contour maps of the normalized variance of stresses between the homogeneous and heterogeneous at 30 days and 366 days with normally distributed young's modulus: (a) according to x axes; (b) according to y axes.

variance in the case when only Young modulus is considered as heterogeneous. As a general observation it is noted that the fluctuation of stresses is amplified because of the spatial variability of the Young's modulus and the variation of temperature and humidity. On the indoor surface the variance is lower in spite of the spatial variability of the mechanical parameter.

This means that the damage due to variation of climate conditions is amplified by the heterogeneous nature of the stone. In Fig. 5, the contour maps represented corresponds to the case when both thermal expansion coefficient and permeability parameter are considered heterogeneous. In spite of the random distribution of these properties, the stress increases towards the outdoor surface with an almost constant gradient and there is very small vertical fluctuations.

Fig. 6 shows the combined effect of the spatial heterogeneity of these three properties in same time. It should be noted that for comparative purposes the same realizations are used in this simulation as in the previous ones from which Figs. 4 and 5 are obtained. It is observed in that case that the point with maximal variance do not coincide with the ones obtained by separated simulations. Moreover, the stress gradient is higher than in the case of previous simulations.

In order to quantify the effect of the variability of the properties on the effective stresses, Fig. 7 compares the three points (EXT2, EXT3 and EXT4) localized at the outdoor surface just as schematized in Fig. 1. This comparison shows that there is no differences between the case where the two parameter E and K are variable (Fig. 7a) and the case with the variability of the three parameters (Fig. 7b). The parameters values attributed at the EXT2 and EXT4 are of the same order for E and K (Fig. 7a). When one adds the variation of the thermal expansion coefficient with the values of 5.77×10^{-6}, 5.86×10^{-6} and 5.76×10^{-6}, respectively for EXT2, EXT3 and EXT4, there is no effect because these values are the same. The differences between the Points EXT2 and EXT3 are caused essentially by the differences between the values of permeability 1.46×10^{-13} and 8.8×10^{-14} m^2, respectively.

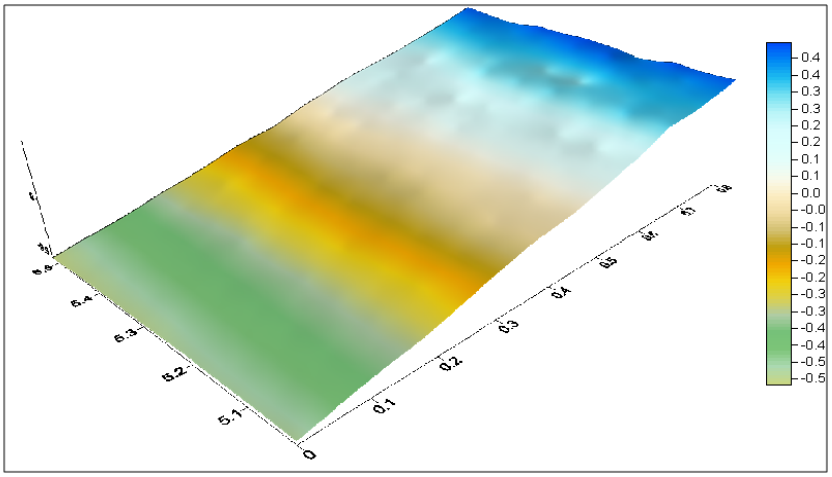

(a)

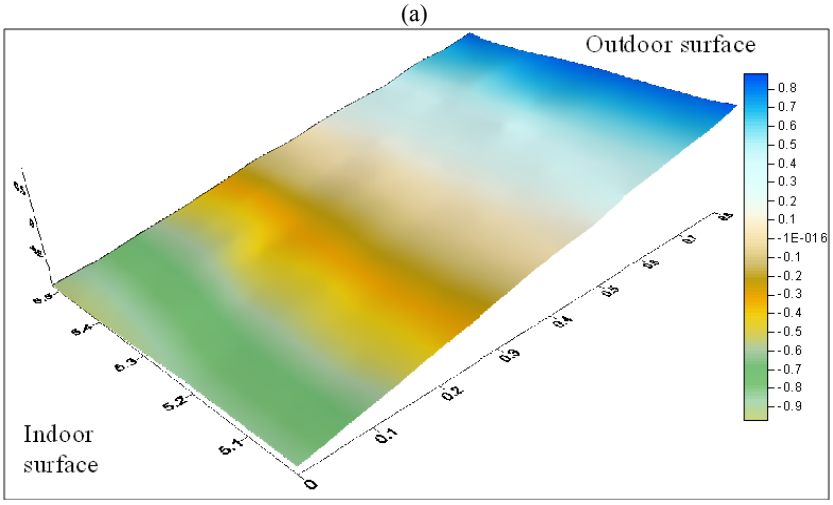

(b)

Fig. 5 Contour maps of the normalized variance of stresses according to y axes at 366 days with the distribution of thermal and hydraulic parameters: (a) with normally distributed thermal expansion coefficient; (b) with normally distributed permeability parameter.

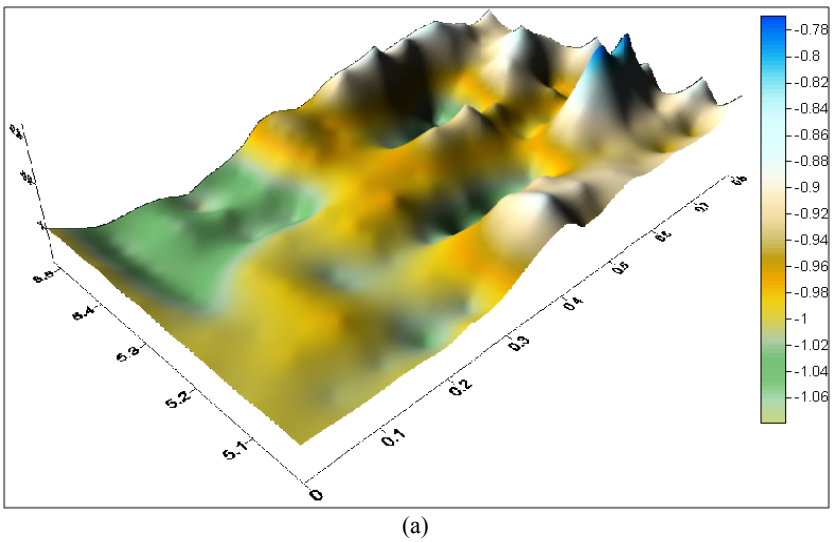

(a)

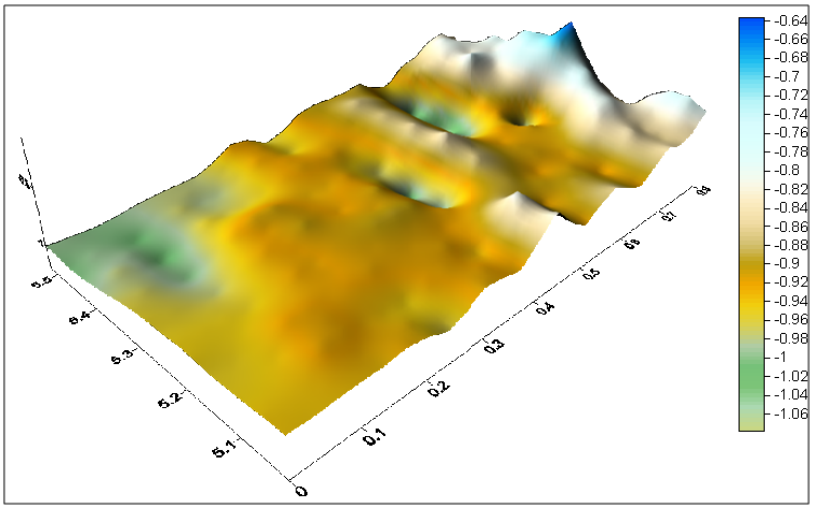

(b)

Fig. 6 Contour maps of normalized variance between homogeneous case and heterogeneous case with considering the three normally distributed parameters: (a) x axes; (b) y axes.

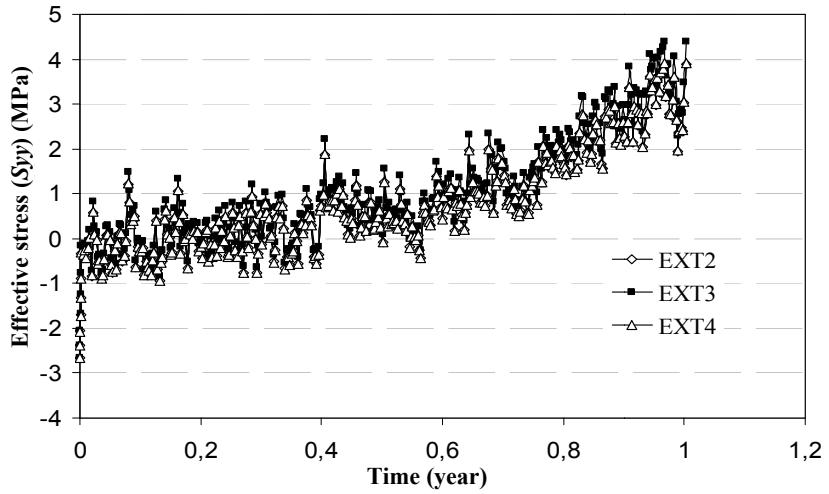

(a)

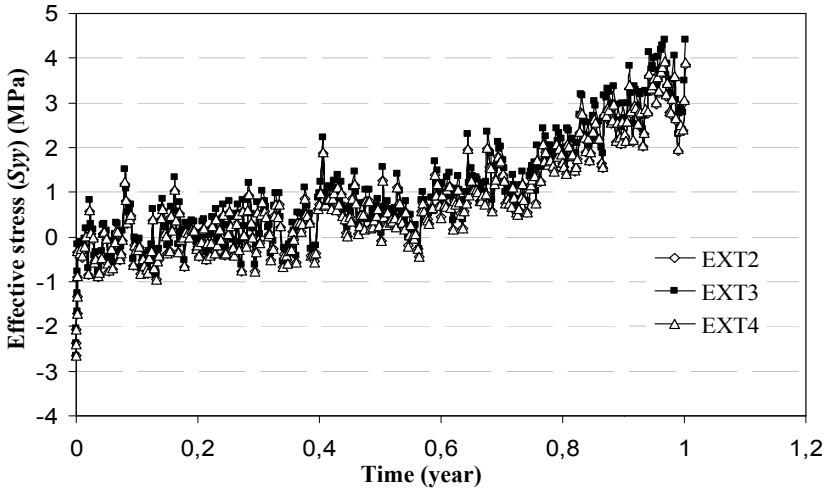

(b)

Fig. 7 Evolution of effective stresses on different points at the outdoor wall surface with: (a) Young modulus and permeability variation; (b) the three parameters variability.

4. Conclusions

An original modeling of building stones behaviour is presented and described in this paper, combining the thermo-hydro-mechanical and geostatistical analysis. The results have shown that the spatial variability of the stone properties has an increasing effect on the fluctuation of stresses due to climate variations. The effect of random distribution of mechanical parameter is greater than the thermal and hydraulic ones. The study highlights the combining factors to initiate and evolve the deterioration of the stone buildings. As the continuity of this study, future work will focus on the fatigue model taking into account the cyclic variation of climatic conditions and spatial variability.

References

[1] Rodriguez-Navarro, C., Doehne, E. 1999. "Salt Weathering: Influence of Evaporation Rate Supersaturation and Crystallization Pattern." *Earth Surface Processes and Landforms* 24: 191-209.

[2] Hoang, H., Hoxha, D., Belayachi, N., and Do, D. P. 2013. "Modelling of Two-Phase Flow in Capillary Porous Medium by a Microscopic Discrete Approach." *European Journal of Environmental and Civil Engineering* 17: 444-52.

[3] Nicholson, D. T., and Nicholson, F. H. 2000. "Physical Deterioration of Sedimentary Rocks Subjected to Experimental Freeze-Thaw Weathring." *Earth Surface Processes and Landforms* 25: 1295-307.

[4] Beck, K. 2006. "Etude des Propriétés. Hydriques et des Mécanismes d'Altération de Pierres Calcaires à Forte Porosité." Ph.D. dissertation, Université d'Orléans. (in French)

[5] Castellanza, R., and Nova, R. 2004. "Oedometric Tests on Artificially Weathered Carbonatic Soft Rocks." *Journal of Geotechnical and Geoenviromental Engineering* 130: 728-39.

[6] Eslami, A., Ronagh, H. R., Mahini, S. S., and Morshed, R. 2012. "Experimental Investigation and Nonlinear FE Analysis of Historical Masonry Buildings—A Case Study." *Construction and Building Material* 35: 251-60.

[7] Carpinteri, A., Invernizzi, S., and Lacidogna, G. 2005. "In Situ Damage Assessment and Nonlinear Modelling of a Historical Masonry Tower." *Engineering Structures* 27: 387-95.

[8] Carpinteri, A., and Lacidogna, G. "Damage Evaluation of Three Masonry Towers by Acoustic Emission." *Engineering Structures* 29: 1569-79.

[9] Verstrynge, E., Schueremans, L., Van Gemet, D., and Hendriks, M. A. N. 2011. "Modelling and Analysis of Time-Dependent Behaviour of Historical Masonry under High Stress Levels." *Engineering Structures* 33:210-7.

[10] Belayachi, N., Hoxha, D., and Do, D. P. 2012. "Thermo-Hydro-Mechanical Behaviour of Tuffeau Stone Masonry." *European Journal of Environmental and Civil Engineering* 16: 1-14.

[11] Warke, P. A., McKinley, J., and Smith, B. J. 2006. "Weathering of Building Stone: Approaches to Assessment, Prediction and Modelling." In *Fracture and Failure of Natural Building Stones,* edited by Kourkoulis, S. K. Dordrecht: Springer Netherlands.

[12] Girard, L., Amitrano, D., and Weiss, J. 2010. "Failure as a Critical Phenomenon in a Progressive Damage Model." *Journal of Statistical Mechanics: Theory and Experiments* 1: 1-13.

[13] Zhang, X. H., Rong, F., Jia, Z. K., Ke, F. J., Xia, M. F., and Bai, Y. L. 2004. "Coupling Effects of Heterogeneity and Stress Fluctuation on Rupture." *Theoretical and Applied Fracture Mechanics* 41: 381-9.

[14] Dyskin, A. 1998. "Stress Fluctuation Mechanism of Mesocrack Growth, Dilatancy and Failure of Heterogeneous Materials in Uniaxial Compression." *HERON* 43: 137-58.

[15] Moropoulou, A., Labropoulos, K., Konstanti, A., Roumpopoulos, K., Bakolas, A., and Michailidis, P. 2006. "Susceptibility of Building Stones to Environmental Loads: Evaluation, Performance, Repair Strategies." In *Fracture and Failure of Natural Building Stones,* edited by Kourkoulis, S. K. Dordrecht: Springer Netherlands.

[16] Vasconcelos, G., and Lourenço, P. B. "Experimental Characterization of Stone Masonry in Shear and Compression." *Construction and Building Materials* 23: 3337-45.

[17] Almeida, C., Paulo, G. J., Arêde, A., Costa, C. Q., and Costa, A. 2012. "Physical Characterization and Compression Tests of One Leaf Stone Masonry Walls." *Construction and Building Materials* 30: 188-97.

[18] Miranda, L. F., Rio, J., Miranda, G. J, and Costa, A. 2012. "Sonic Impact Method—A New Technique for Characterization of Stone Masonry Walls." *Construction and Building Materials* 36: 27-35.

[19] Chau, K, T., and Shao, J. F. 2006. "Subcritical Crack Growth of Edge and Center Cracks in Façade Rock Panels Subject to Periodic Surface Temperature Variations." *International Journal of Solids and Structures* 43: 807-27.

[20] Chavant, C. 2009. "Modèles de Comportement THHM." Code_Aster. Accessed June 20, 2011. http://code-aster.org/doc/v10/fr/man_r/r7/r7.01.11.pdf. (in French)

[21] Coussy, O. 1995. *Mechanics of Porous Continua.* New York: Wiley Ltd.

[22] Lopez, D. L., and Smith, L. 1996. "Fluid Flow in Fault Zones: Influence of Hydraulic Anisotropy and Heterogeneity on the Fluid and Heat Transfer Regime." *Water Resources Research* 32: 3227-35.

[23] Schulz, S. E., and Evans, J. P. 2000. "Mesoscopic Structure of the Punchbowl Fault, Southern California and the Geologic and Geophysical Structure of Active Strike-Slip Faults." *Journal of Structural Geology* 22: 913-30.

[24] McKinley, J., Warke, P., Lloyd, C. D., Ruffell, A. H., and Smith, B. J. 2006. "Geostatistical Analysis in Weathering Studies: Case Study for Stanton Moor Building Sandstone." *Earth Surface Processes and Landforms* 31: 950-69.